



# Flat-top optical resonance in a single-ring resonator based on manipulation of fast- and slow-light effects

MENGHAO HUANG,<sup>1</sup> SIMIN LI,<sup>1,2</sup> MIN XUE,<sup>1</sup> LEI ZHAO,<sup>1</sup> AND SHILONG PAN<sup>1,3</sup>

<sup>1</sup>Key Laboratory of Radar Imaging and Microwave Photonics, Ministry of Education, Nanjing University of Aeronautics and Astronautics, Nanjing 210016, China

<sup>2</sup>lisimin@nuaa.edu.cn

<sup>3</sup>pans@nuaa.edu.cn

**Abstract:** Optical single-ring resonance inherently generates Lorentzian-shape magnitude and group-delay responses, leading to critical performance limitation in photonics, cavity quantum electrodynamics, cavity optomechanics, and atomic and optical physics. Here, we propose a new type of microresonator that stimulates flat-top resonance in a single-ring cavity. By manipulating the fast and slow light effects in the microresonator, the flat-top group delay can be tuned with an ignorable magnitude variation. In addition, the bandpass response can be switched to a notch, which can enable function-reconfigurable photonic integrated circuits (PICs) without a physical change in the architecture. Our demonstration provides the possibility of developing microresonator-based PICs with unprecedented high flexibility and capacity.

© 2018 Optical Society of America under the terms of the [OSA Open Access Publishing Agreement](#)

## 1. Introduction

Because of the capability to manipulate the magnitudes and phases of optical signals within a very small footprint [1], optical microring resonators (MRR) are regarded as fundamental building blocks of photonic integrated circuits (PICs), which pave the way to implement lasers [2], modulators [3], amplifiers [4], sensors [5], filters [6], optical add/drop multiplexers [7], switches [8], logic gates [9], delay lines [10], optical buffers [11], optical frequency comb generators [12], and even photonic subsystems [13] in an ultra-small chip. A generic MRR consists of a looped optical waveguide that enables a series of resonant modes and one or two waveguides to access these modes [14]. Since the resonant optical wavelengths can be circulated in the ring for a long time, the physical length for controlling the properties of those wavelengths is dramatically shortened. However, the cavity resonance intrinsically stimulates a Lorentzian magnitude response with a very sharp peak, which also leads to a spike in the group-delay spectrum; therefore, the bandwidth or information handling capacity of the MRR is inherently limited. To manipulate the magnitude and phase of a wideband signal, a number of MRRs connected in series or parallel need to be applied. For instance, five series-coupled MRRs were used to implement an integrated optical filter with a 3-dB bandwidth of 1.9 GHz and a free spectral range (FSR) of 50 GHz [15] and 40 MRRs were cascaded to produce a tunable time delay of 535 ps in a bandwidth of 20 GHz [16]. The use of multiple MRRs not only occupies a larger chip area but also dramatically increases the insertion loss, transmission latency, and difficulty of fabrication. In addition, a very large number of parameters, such as the coupling coefficients and the optical lengths of the MRRs, have to be precisely adjusted to synthesize the broad bandwidth, resulting in extreme difficulties in controlling. The difficulties would further increase if the system has to be tunable. Another drawback of the conventional MRR is that the group-delay response is closely related to the magnitude response [17] due to the well-known Kramers–Kronig relation and, therefore, the tuning of the group delay can lead to intensity variations in the order of tens of dBs. For cascaded MRRs, the tight coupling between the magnitude and the phase responses also results in a magnitude ripple of 25–30 dB for a given group delay [11].

Moreover, PICs-based MRRs always have no or very limited reconfigurability because the through (or drop) port of an MRR can only achieve a notch (or bandpass) response, and a switch between the two responses for a given port is impossible. Therefore, although the conventional MRRs have a simple structure, they will practically count against large-scale, low cost, and on-chip reconfigurable photonic integration if serving as fundamental building blocks for wideband PICs.

In this paper, we propose a new type of optical microring resonator that stimulates flat-top resonance to enable the capability of manipulating the magnitudes and phases of wideband optical signals. Compared with the conventional MRR, the footprint of the flat-top microring resonator (FTMRR) is nearly unchanged because only an optical reflector is added that can be very small [18], while the bandwidths of the magnitude response with a 0.5-dB ripple and the group-delay response with 1-ps ripple are dramatically increased. By simply manipulating the fast- and slow-light effects in the FTMRR, the flat-top group delay can be tuned in a range of more than 100 ps with a magnitude variation of less than 0.8 dB. In addition, the response of the FTMRR can be switched flexibly between a bandpass response and a notch response depending on which effect is dominant.

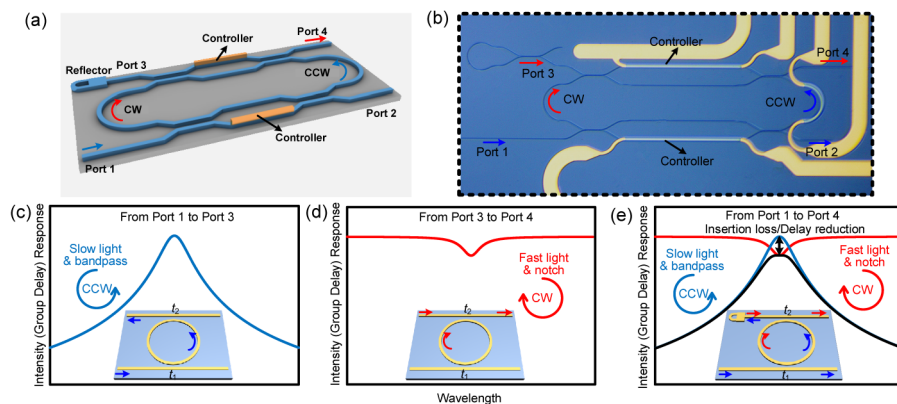


Fig. 1. Schematic and representative responses of the FTMRR. (a), (b) Architecture of the device, which includes a microring and a reflector. The controllers are used to control the self-coupling coefficients. (c), (d), (e) Principle of achieving broadband resonance. In the FTMRR, strong slow light (or bandpass response) and weak fast light (or notch response) around the resonant wavelength can be generated simultaneously in the ring cavity along the CCW and CW directions, respectively, so that the entire resonance results in a flat-top magnitude and group-delay responses.

## 2. Methods

The FTMRR is illustrated in Fig. 1(a) and 1(b), which consists of a conventional add-drop MRR with a reflector (e.g., waveguide grating, metal film, or loop mirror) in the drop port. Input light satisfying the resonant condition couples into the MRR cavity through the lower coupler and propagates in the counterclockwise (CCW) direction. At the upper coupler, a portion of the resonant light couples out to the drop port and is then reflected back into the cavity by the reflector, circulates in the clockwise (CW) direction, and finally exits from Port 3. We assume that the light intensity in the CCW and CW modes can only stimulate an ignorable nonlinear interaction; therefore, the propagation in the two directions can be seen as independent. By properly setting the coupling coefficients, a strong slow-light effect is obtained in the CCW mode, and a weak fast-light effect occurs in the CW mode, as shown in Fig. 1(c) and 1(d). The combination of the two effects creates a flat-top resonance, as shown in Fig. 1(d), resulting in broadband magnitude and group-delay responses. The amplitude transmission and group delay response of the FTMRR shown in Fig. 1(e) is given by

$$E_4 = \frac{\eta \sqrt{a} k_1 k_2 e^{\frac{i\phi}{2}} (t_2 - at_1 e^{i\phi})}{(1 - at_1 t_2 e^{i\phi})^2} E_1 \quad (1)$$

$$\tau = \left[ \frac{1}{2} + \frac{a^2 t_1^2 - at_1 t_2 \cos \phi}{a^2 t_1^2 + t_2^2 - 2at_1 t_2 \cos \phi} + \frac{2(at_1 t_2 \cos \phi - a^2 t_1^2 t_2^2)}{1 + a^2 t_1^2 t_2^2 - 2at_1 t_2 \cos \phi} \right] \frac{n_g L}{c} \quad (2)$$

where  $E_1$  is the incident field,  $\phi = \beta L$  is the single-pass phase shift,  $L = 2\pi r$ ,  $r$  is the radius of the microring,  $\beta$  is the propagation constant of the circulating mode,  $a$  is the single-pass amplitude transmission coefficient,  $t_1$ ,  $t_2$  are the self-coupling coefficients, and  $k_1$ ,  $k_2$  are the cross-coupling coefficients.  $\eta$  represents the transmission loss induced by the reflectivity of the reflector. The flat-top group-delay response is achieved when  $d^2\tau/d(\cos\phi)^{2=0}$ , leading to

$$t_2 = (1 + 2^{0.2} at_1) / (2^{0.2} + at_1) \quad (3)$$

As can be seen, there is a one-to-one mapping between  $t_1$  and  $t_2$  to satisfy the flat-top state. The practical applications could tolerate a certain group delay variation (e.g., 1 ps) so that the values of  $t_1$  and  $t_2$  could slightly deviate from the ideal values to achieve the largest 1-ps bandwidth. Similarly, a flat-top intensity response can be achieved. It should be noted that in [19] backscattering in silicon microrings was discussed while it is considered as problems for applications. In [20-21] CCW and CW modes are used to mitigate resonance while flat-top response or group delay are not realized to broaden the resonance bandwidth.

### 3. Experimental results

The FTMRR can be fabricated using typical optical waveguide materials, such as silicon on insulator (SOI), polymer, indium phosphide, lithium niobate, and so on. In this study, we fabricated the FTMRR using a silicon nitride TriPleX<sup>TM</sup> waveguide platform [22]. We use a Mach-Zehnder structure to adjust the coupling coefficient, which can achieve a wide tuning range. This structure, however, would occupy a relatively large footprint, so the ring cavity is 4293.9  $\mu\text{m}$  long. The group index is 1.71, corresponding to an FSR of 0.3272 nm. Thermo-optic heaters are deposited in the lower and upper coupling regions, as shown in Fig. 1(a). Based on the thermo-optic effect, the coupling coefficients can be adjusted by changing the bias voltages to the electrodes. Other coupling coefficient-tuning mechanisms such as free-carrier injection [3] and the electro-optic effect [23] can also be applied. The group delay and magnitude responses of the device are measured by an optical vector analyzer (OVA) with 1-MHz spectral resolution based on optical single-sideband modulation [24].

Figure 2 shows the simulated and measured group-delay and magnitude responses for a fixed  $t_1$  and a varied  $t_2$ . The experimental results coincide well with the numerical calculation based on the model in [17], which indicates that we can evaluate the parameters of the fabricated FTMRR, such as  $t_1$ ,  $t_2$ , and the single-pass amplitude transmission coefficient  $a$  based on the fitting results. As shown in Fig. 2(a), when  $t_2$  is near  $at_1$ , there is a deep notch in the group delay response because the fast light in the CW mode is dominant and the output resonant light is a strong fast light. With the increase in  $t_2$ , the fast light weakens, and the slow light in the CCW mode almost remains the same, so that the notch in the group delay response is small. Broadband and flat-top group-delay responses are eventually achieved with a very small ripple. When  $t_2$  is increased further, the strong slow light causes the flat-top group delay to return to the Lorentzian shape. Figure 2(b) shows the intensity responses, which vary similarly to the group-delay responses, i.e., changing from a notch response to a bandpass response with the increase of  $t_2$ . The flat-top shape is achieved with parameters close to those for a flat-top group-delay response. Figure 2(b) also indicates that the FTMRR not only serves as a flat-top delay device, but also implements shape-reconfigurable optical filtering, high-extinction-ratio optical switching, high-efficiency intensity modulation, or high-sensitivity sensing.

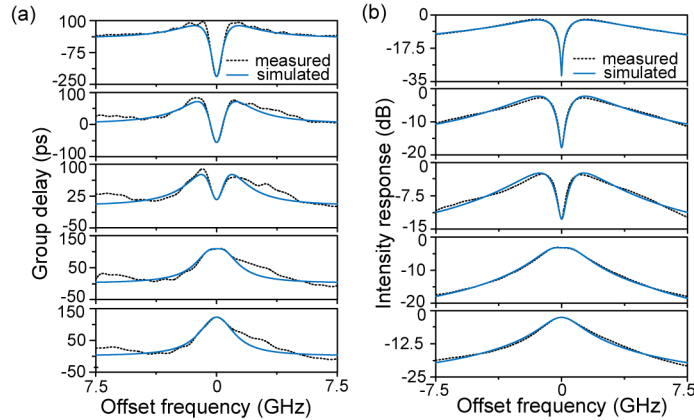


Fig. 2. Tuning of the delay and intensity responses of the FTMRR using one self-coupling coefficient while keeping the other unchanged. (a) The measured/simulated group delays show the change from fast to slow light. For a certain coupling coefficient, a flat-top group-delay response can be obtained. (b) The measured/simulated group delays show the change from a notch response to a bandpass response. A flat-top intensity response can also be obtained with specific coupling coefficients.

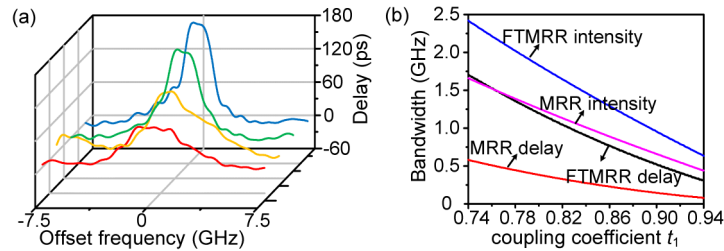


Fig. 3. The group delays of the proposed FTMRR tuned by adjusting the coupling coefficients of the lower and upper coupling regions. (a) The measured group-delay responses. (b) The calculated bandwidths of the delay (with 1-ps ripple) and intensity (with 0.5-dB ripple) responses for the FTMRR and the conventional MRR with the same parameters.

The flat-top responses can be tuned by adjusting  $t_1$  and  $t_2$ , as shown in Fig. 3(a). The measured group delays for the four flat-tops are 73, 110, 159, and 180 ps, respectively. The in-band ripple is mainly due to the group-delay response measurement methods, which demand a high-phase measurement accuracy in the differential calculation [24], while the vibration and temperature in the laboratory environment could not guarantee a negligible phase drift. Figure 3(b) shows the calculated relationship between the delay and bandwidth of the FTMRR. For comparison, the simulated results of the conventional MRR with the same parameters, except for the reflector, are shown as well. When the coupling coefficient  $t_1$  is tuned in the range from 0.74 to 0.94, the value of the group delay for the FTMRR can be tuned from 50.8 to 188 ps, and the bandwidth with 1-ps ripple ranges from 0.31 to 1.7 GHz. For the conventional MRR with the same coupling coefficients, the delay-bandwidth is only 1/2.2 to 1/2.9 of the FTMRR. Meanwhile, the bandwidth for the intensity response with 0.5-dB flatness is 2.42 to 0.63 GHz for the FTMRR and 1.66 to 0.44 GHz for the MRR.

The intensity responses for the flat-top group delays are bandpass with small insertion losses. In comparison, most conventional MRR-based on-chip delay lines output signals from the through port, introducing an intrinsic loss of tens of dB and a considerable intensity variation for delay tuning because the intensity response at the through port is a notch [11]. The insertion losses of the intensity responses for the flat-top group delays shown in Fig. 3(a) is also measured with the fiber coupling losses excluded, of which the variation is less than 0.8 dB during the more than 100-ps group-delay tuning range. This exciting feature is

achieved because a larger group delay requires an enhanced slow-light effect in the CCW propagation, which leads to a sharper peak in the group-delay response and a lower transmission loss in the peak. To flatten the group delay, the fast-light effect in the CW propagation should also be enhanced, corresponding to a more significant transmission loss in the notch. As a result, the increase in the transmission loss in the CW propagation can be partly compensated for by the transmission loss reduction in the CCW propagation, leading to a smaller loss variation for delay tuning. It should be noted that small phase-intensity dependence is highly desired for wideband reconfigurable photonic systems such as photonic microwave filters [25], optical signal processors [26], and optical beamformers [27], which saves at least one on-chip attenuator and the corresponding control circuit [22]. This feature would greatly simplify the MRR-based PICs which may integrate thousands of MRRs.

Because the group-delay response and the intensity response have similar shapes at Port 4, the flat-top intensity response can also be achieved by proper selection of the coupling coefficients, and the bandwidth can be tuned when different coupling coefficients are applied, as shown in Fig. 4. This flat-top and bandwidth-tunable optical intensity response is very useful for optical signal processing [26].

Similar to the MRR, cascading the FTMRs is an efficient way to further improve the optical magnitude and phase manipulation capabilities such as bandwidth, extinction ratio, and tuning range.

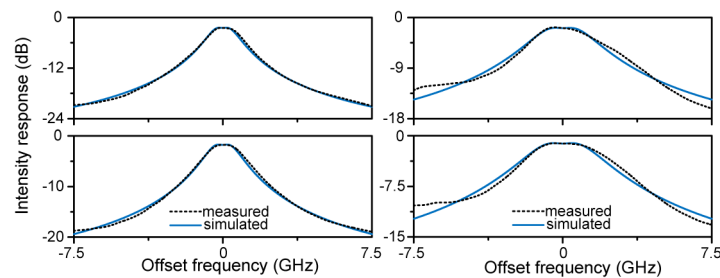


Fig. 4. The measured bandwidth-tunable flat-top bandpass responses of the proposed FTMR when the coupling coefficients are adjusted.

#### 4. Conclusions

In conclusion, we have proposed and demonstrated a new microring resonator with flat-top responses based on manipulating the slow- and fast-light effects. This new architecture not only breakthroughs the classic physics limitation that single ring resonance can only generate Lorentzian-shape magnitude and group-delay responses, but also enables small phase-intensity dependence and switching between the bandpass and notch responses without changing the physical architecture, which was impossible for conventional single-ring resonators. Therefore, the proposed FTMR could provide MRR-based PICs with significantly improved reconfigurability and bandwidth, as well as substantially reduced size. The proposed FTMR is also expected to offer numerous prospects for other types of resonant systems, which are widely applied in photonics, cavity quantum electrodynamics, optomechanics, and atomic and optical physics.

#### 5. Funding

National Natural Science Foundation of China (61527820 and 61604072), and the Fundamental Research Funds for the Central Universities (NC2018005).

#### References

1. Q. Xu, D. Fattal, and R. G. Beausoleil, "Silicon microring resonators with 1.5- $\mu\text{m}$  radius," *Opt. Express* **16**(6), 4309–4315 (2008).

2. M. Kues, C. Reimer, B. Wetzel, P. Roztocki, B. E. Little, S. T. Chu, T. Hansson, E. A. Viktorov, D. J. Moss, and R. Morandotti, "Passively mode-locked laser with an ultra-narrow spectral width," *Nat. Photonics* **11**(3), 159–162 (2017).
3. A. Biberman, E. Timurdogan, W. A. Zortman, D. C. Trotter, and M. R. Watts, "Adiabatic microring modulators," *Opt. Express* **20**(28), 29223–29236 (2012).
4. S. Hua, J. Wen, X. Jiang, Q. Hua, L. Jiang, and M. Xiao, "Demonstration of a chip-based optical isolator with parametric amplification," *Nat. Commun.* **7**, 13657–13662 (2016).
5. H. H. Zhu, Y. H. Yue, Y. J. Wang, M. Zhang, L. Y. Shao, J. J. He, and M. Y. Li, "High-sensitivity optical sensors based on cascaded reflective MZIs and microring resonators," *Opt. Express* **25**(23), 28612–28618 (2017).
6. J. S. Fandiño, P. Muñoz, D. Doménech, and J. Capmany, "A monolithic integrated photonic microwave filter," *Nat. Photonics* **11**(2), 124–129 (2017).
7. S. Wang, X. Feng, S. Gao, Y. Shi, T. Dai, H. Yu, H. K. Tsang, and D. Dai, "On-chip reconfigurable optical add-drop multiplexer for hybrid wavelength/mode-division-multiplexing systems," *Opt. Lett.* **42**(14), 2802–2805 (2017).
8. V. R. Almeida, C. A. Barrios, R. R. Panepucci, and M. Lipson, "All-optical control of light on a silicon chip," *Nature* **431**(7012), 1081–1084 (2004).
9. Q. Xu and M. Lipson, "All-optical logic based on silicon micro-ring resonators," *Opt. Express* **15**(3), 924–929 (2007).
10. J. Capmany, I. Gasulla, and S. Sales, "Microwave photonics: Harnessing slow light," *Nat. Photonics* **5**(12), 731–733 (2011).
11. F. Xia, L. Sekaric, and Y. Vlasov, "Ultracompact optical buffers on a silicon chip," *Nat. Photonics* **1**(1), 65–71 (2007).
12. X. Xue, Y. Xuan, Y. Liu, P.-H. Wang, S. Chen, J. Wang, D. E. Leaird, M. Qi, and A. M. Weiner, "Mode-locked dark pulse Kerr combs in normal-dispersion microresonators," *Nat. Photonics* **9**(9), 594–600 (2015).
13. W. Liu, M. Li, R. S. Guzzon, E. J. Norberg, J. S. Parker, M. Lu, L. A. Coldren, and J. Yao, "A fully reconfigurable photonic integrated signal processor," *Nat. Photonics* **10**(3), 190–195 (2016).
14. W. Bogaerts, P. D. Heyn, T. V. Vaerenbergh, K. D. Vos, S. K. Selvaraja, T. Claes, P. Dumon, P. Bienstman, D. V. Thourhout, and R. Baets, "Silicon microring resonators," *Laser Photonics Rev.* **6**(1), 47–73 (2012).
15. P. Dong, N.-N. Feng, D. Feng, W. Qian, H. Liang, D. C. Lee, B. J. Luff, T. Banwell, A. Agarwal, P. Toliver, R. Menendez, T. K. Woodward, and M. Asghari, "GHz-bandwidth optical filters based on high-order silicon ring resonators," *Opt. Express* **18**(23), 23784–23789 (2010).
16. P. A. Morton, J. B. Khurgin, Z. Mizrahi, and S. J. Morton, "Commercially packaged optical true-time-delay devices with record delays of wide bandwidth signals," In *CLEO 2014, OSA Technical Digest*, paper AW3P.6.
17. J. Heebner, R. Grover, and T. Ibrahim, *Optical microresonators: theory, fabrication, and applications* (Springer, 2008).
18. M. W. Pruessner, T. H. Stievater, and W. S. Rabinovich, "Integrated waveguide Fabry-Perot microcavities with silicon/air Bragg mirrors," *Opt. Lett.* **32**(5), 533–535 (2007).
19. A. Li, T. V. Vaerenbergh, P. D. Heyn, P. Bienstman, and W. Bogaerts, "Backscattering in silicon microring resonators: a quantitative analysis," *Laser Photonics Rev.* **10**(3), 420–431 (2016).
20. Q. Li, Z. Zhang, J. Wang, M. Qiu, and Y. Su, "Fast light in silicon ring resonator with resonance-splitting," *Opt. Express* **17**(2), 933–940 (2009).
21. A. Li and W. Bogaerts, "An actively controlled silicon ring resonator with a fully tunable Fano resonance," *APL Photonics* **2**(9), 096101 (2017).
22. C. G. H. Roeloffzen, L. Zhuang, C. Taddei, A. Leinse, R. G. Heideman, P. W. van Dijk, R. M. Oldenbeuving, D. A. I. Marpaung, M. Burla, and K.-J. Boller, "Silicon nitride microwave photonic circuits," *Opt. Express* **21**(19), 22937–22961 (2013).
23. A. Guarino, G. Poberaj, D. Rezzonico, R. Degl'Innocenti, and P. Günter, "R. Degl'Innocenti, and P. Günter, "Electro-optically tunable microring resonators in lithium niobate," *Nat. Photonics* **1**(7), 407–410 (2007).
24. S. L. Pan and M. Xue, "Ultrahigh-resolution optical vector analysis based on optical single-sideband modulation," *J. Lightwave Technol.* **35**(4), 836–845 (2017).
25. D. Pastor, J. Capmany, B. Ortega, A. Martinez, L. Pierno, and M. Varasi, "Reconfigurable RF photonic filter with negative coefficients and flat-top resonances using phase inversion in a newly designed 2×1 integrated Mach-Zehnder modulator," *IEEE Photonics Technol. Lett.* **16**(9), 2126–2128 (2014).
26. J. Capmany, I. Gasulla, and D. Pérez, "Microwave Photonics: The programmable processor," *Nat. Photonics* **10**(1), 6–8 (2016).
27. M. Burla, D. A. I. Marpaung, L. Zhuang, M. R. Khan, A. Leinse, W. Beeker, M. Hoekman, R. G. Heideman, and C. G. H. Roeloffzen, "Multiwavelength-Integrated Optical Beamformer Based on Wavelength Division Multiplexing for 2-D Phased Array Antennas," *J. Lightwave Technol.* **32**(20), 3509–3520 (2014).